Applied Catalysis B: Environmental 166–167 (2015) 497–508

Contents lists available at ScienceDirect

Applied Catalysis B: Environmental

journal homepage: www.elsevier.com/locate/apcatb

Iron oxides semiconductors are efficients for solar water disinfection: A comparison with photo-Fenton processes at neutral pH

C. Ruales-Lonfat[a], J.F. Barona[b], A. Sienkiewicz[c], M. Bensimon[d], J. Vélez-Colmenares[a], N. Benítez[b], C. Pulgarín[a,*]

[a] SB, ISIC, GPAO, Station 6, Ecole Polytechnique Fédérale de Lausanne, 1015 Lausanne, Switzerland
[b] Universidad del Valle, Grupo de Investigación en Procesos Avanzados de Oxidación (GAOX), Cali AA 25360, Colombia
[c] SB, IPMC, LPMC, Station 3, Ecole Polytechnique Fédérale de Lausanne, 1015 Lausanne, Switzerland
[d] ENAC-IIEGR-CEL, Station 18, Ecole Polytechnique Fédérale de Lausanne, 1015 Lausanne, Switzerland

ARTICLE INFO

Article history:
Received 10 October 2014
Received in revised form 1 December 2014
Accepted 3 December 2014
Available online 6 December 2014

Keywords:
Iron (hydr)oxide
Bacterial inactivation
Semiconductors
Heterogeneous photo-Fenton
Photo-Fenton at neutral pH

ABSTRACT

The photocatalytic activities of four different commercially available iron (hydr)oxides semiconductors, *i.e.* hematite (α-Fe_2O_3), goethite (α-FeOOH), wüstite (FeO) and magnetite (Fe_3O_4), were evaluated for bacteria inactivation at neutral pH in the absence or presence of H_2O_2. Our results showed that heterogeneous photocatalysis and/or photo-Fenton processes catalyzed by low concentrations of reagents (0.6 mg/L Fe^{3+} and 10 mg/L H_2O_2) under sunlight may serve as a disinfection method for waterborne bacterial pathogens. In particular, we found that, with the exception of magnetite which need H_2O_2 as electron acceptor, all the other semiconductor iron (hydr)oxides were photoactive under sunlight in absence of H_2O_2 (using only oxygen as electron acceptor). Furthermore, for all iron (hydr)oxide studied in this work, no bacterial reactivation and/or growth was observed after photo-Fenton treatment. The same antimicrobial activity was obtained for the photocatalytic semiconducting action of hematite and goethite. Additionally, a delayed disinfection effect was observed to continue in the dark for the photo-assisted wüstite-based treatment. Electron spin resonance (ESR) in combination with spin-trapping was employed to detect reactive oxygen species (ROS) involved in heterogeneous photocatalysis and/or photo-Fenton treatments mediated by iron (hydr)oxide particles. In particular, ESR confirmed that $^{\bullet}OH$ and $O_2^{\bullet-}$ radicals were the principal ROS produced under photo-assisted action of iron (hydr)oxide particles in the absence or presence of H_2O_2. We also found that the components of natural water (*i.e.* natural organic matter (NOM) and inorganic substances) did not interfere with the photocatalytic semiconducting action of hematite to bacterial inactivation. However, these components enhance the bacterial inactivation by heterogeneous photo-Fenton action of hematite.

Overall our results demonstrated, for the first time, that low concentration of iron (hydr)oxides, acting both as photocatalytic semiconductors or catalysts of the heterogeneous photo-Fenton process at neutral pH, may provide a useful strategy for efficient bacterial disinfection.

1. Introduction

Drinking water scarcity is one of the most serious global challenges of our time [1,2]. The necessity for advanced water purification in terms of eliminating contaminants and killing bacteria will continue to increase, especially in developing countries where water treatment is often inadequate or non-existent. The photo-assisted Fenton oxidation is one of the most popular and widely studied advanced oxidation processes (AOPs). In particular, photo-Fenton reactions play a key role in sunlight-assisted AOPs due to the fact that they take advantage of UV, near-UV and visible light up to 600 nm, thus comprising 35% of the total energy coming from the solar spectrum. Until now, the pH of the process was generally perceived as the limiting factor for photo-Fenton systems, because $Fe(OH)^{2+}$, *i.e.* the most photo-active Fe^{3+}-hydroxy complex under UV-A and visible solar light, is predominant at low pH (~2.8) [3,4]. However, recently, the photo-inactivation of *E. coli* by photo-Fenton system at near neutral pH has been reported [5–10]. A near neutral pH, a spontaneous chemical oxidation of ferrous ions to ferric by dissolved oxygen in water occurs, involving a variety of partially oxidized meta-stable ferrous–ferric intermediate species (*e.g.* green rusts). These iron intermediates ultimately transform

* Corresponding author. Tel.: +41 21 693 47 20; fax: +41 21 693 6161.
E-mail address: cesar.pulgarin@epfl.ch (C. Pulgarín).

http://dx.doi.org/10.1016/j.apcatb.2014.12.007
0926-3373/

into a variety of stable iron oxide end-products such as hematite, magnetite, goethite and lepidocrocite [11,12].

Recent researches haves focused on the idea of replacing dissolved iron with solid catalysts in so-called heterogeneous Fenton reactions. In particular, quite a number of iron-containing systems have been developed for organic pollutants degradation, including iron oxides [13–15], iron-immobilized materials [16–18], clays and carbon materials [19,20], *etc.*

Iron oxides are among the most chemically reactive components of suspended matter in aquatic systems and can be easily prepared in laboratory conditions [21]. Additionally, they are considered non-toxic and environmentally friendly compounds, similarly to free iron ions [22]. Most of them reveal semiconductor properties and then may also act as photocatalysts, even though their overall efficacy can be impaired by a very efficient hole–electron recombination [23].

Possible semiconducting mechanisms involved in iron oxide can be summarized as follows. In the first step, a photon with energy equal to or greater than the material's band gap, which separates the conductance band (CB) and valence band (VB), is absorbed by a semiconducting particle of iron oxide. This gives rise to the generation of the electron/hole pair (Eq. (1)). Although the excited electron/hole pair can recombine and release the energy as heat, some of the excited electrons and holes can contribute to redox reactions on the surface of a semiconducting particle of iron oxide. The most relevant redox processes, which take place after the photo-generation of electrons (e^-_{cb}) and holes (h^+_{vb}) in semiconducting particles of iron oxide suspended in aqueous medium, containing also an organic substance (RX), are summarized in Eqs. (1)–(5) [21]. ($>Fe^{2+}$ and $>Fe^{3+}$ represent the Fe^{2+}/Fe^{3+} species in solid or solution phase).

$$Fe_2O_3 + h\nu \rightarrow Fe_2O_3\,(e^- + h^+) \quad (1)$$

$$e^-_{(cb)} + O_2 \rightarrow O_2^{\bullet -} \quad (2)$$

$$h^+_{(vb)} + O_2^{\bullet -} \rightarrow {}^1O_2 \quad (3)$$

$$e^-_{(cb)} + {>}Fe^{3+} \rightarrow {>}Fe^{2+} \quad (4)$$

$$h^+_{(vb)} + RX_{ad} \rightarrow RX_{ad}^{\bullet +} \quad (5)$$

Irradiation may also enhance the heterogeneous Fenton process on iron-bearing particles, by promoting the photo-reduction of $>Fe^{3+}OH$ to $>Fe^{2+}$ (Eq. (6)), which subsequently reacts with H_2O_2 generating $^\bullet OH$ radicals at the particle surface (Eq. (7)).

$${>}Fe^{3+}OH + h\nu \rightarrow {>}Fe^{2+} + {}^\bullet OH \quad (6)$$

$${>}Fe^{2+} + H_2O_2 \rightarrow {>}Fe^{3+} + OH^- + {}^\bullet OH \quad (7)$$

A large number of studies have demonstrated that iron oxide minerals such as magnetite, hematite, goethite or ferrihydrite are effective for oxidation of organic pollutants and compounds that affect water quality [13,14,24–26]. However, since little research has been conducted on these compounds towards inactivation of microorganisms present in aqueous solutions [7,17,27–29], their role in bacterial inactivation is not well known. In our previous paper [7], it was shown that goethite was efficiently inactivating bacteria, acting as semiconductor *via* a photocatalytic process and as an heterogeneous iron source in Fenton process around neutral pH.

In this work, the bacterial inactivation by addition of $FeSO_4$ in illuminated water at initial pH of 6.5 and 7.5 were compared in the absence or presence of H_2O_2. Also, the ferric precipitates formed during the treatments were identified.

The main purpose of this work was to investigate the disinfection ability of four iron (hydr)oxides in aqueous media under solar light illumination, at near-neutral pH of 6.5, in the absence or presence of H_2O_2, to better distinguish their action mode, either as semiconductors or as iron source in heterogeneous photo-Fenton processes. The iron (hydr)oxide (hematite, goethite, wüstite and magnetite) used in this study are the most common constituents of the sub-surface environment. Furthermore, reactive oxygen species (ROS) generated by iron (hydr)oxides during these processes were identified and quantified. Finally, the influence of natural organic matter (NOM) on the activity of hematite during bacterial inactivation was evaluated.

2. Materials and methods

2.1. Chemicals

Ferrous sulphate heptahydrate ($FeSO_4{\cdot}7H_2O$) (Riedel-de Haën 99–103.4%), hydrogen peroxide (H_2O_2) 30% w/v (Riedel de Haën). Sodium hydroxide (NaOH, 98%) and hydrochloric acid (HCl, 36.5%), were purchased from Sigma-Aldrich. The spin-trap, 5,5-dimethyl-1-pyrroline-N-oxide (DMPO), was purchased from Enzo Life Sciences (ELS) AG (Lausen, Switzerland). The spin probes, 4-hydroxy-2,2,6,6-tetramethylpiperidine-1-oxyl (TEMPOL) and 4-oxo-2,2,6,6-tetramethylpiperidine-1-oxyl (TEMPONE), as well as their respective precursors, *i.e.* 2,2,6,6-tetramethyl-4-piperidinol (TMP-OH) and 2,2,6,6-tetramethyl-4-piperidone (TEMPONE precursor), were purchased from Sigma Aldrich (Buchs, Switzerland). The commercially available iron (hydr)oxides particles, *i.e.* goethite, hematite, wüstite, and magnetite, were purchased from Sigma-Aldrich. The particles size were (<50 mesh and <5 μm). The most relevant physicochemical properties of these iron (hydr)oxides particles are shown in Table 1.

All solutions were prepared immediately prior to irradiation with the use of Milli-Q water (18.2 MΩ-cm). Two different types of water were used to suspend bacteria that are Milli-Q water and natural water from the Geneva Lake. Table 2 shows the physicochemical characteristics of these waters.

2.2. Bacterial strains and growth media

The bacterial strain used was *E. coli* K12 (MG1655), a non-pathogenic wild-type strain, which can be handled with little genetic manipulation. Bacteria was inoculated from a stock in a

Table 1
Physicochemical properties of the particles studied.

Iron minerals	Formula	Iron oxidation state	Surface area (m^2/g)[a]	IEP[b]	Band gap energy[b] (eV)
Goethite	α-FeOOH	+3	37.0	7.5–8.5	2.1
Hematite	α-Fe_2O_3	+3	–	8.5	2.2
Wüstite	FeO	+2	10.0	8.0	2.4
Magnetite	Fe_3O_4	+2, +3	2.0	6.0–6.5	0.1

[a] Surface area reported by the manufacturer and from references [14,66].
[b] Isoelectric point and band gap energy, from references [21,60].

Table 2
Physicochemical characteristics of the waters used in the experiments.

Parameter	Milli-Q water	Geneve lake water
Conductivity at 20 °C (μS/cm)	<0.055	252
Transmittance at 254 nm (%)	100	96
pH	6.5	7.9
Total organic carbon (TOC) (mg C/L)	<0.005	0.8–1
Iron (mg/L)	–	0.019
Phosphates	–	0.012
Hydrogen carbonate (mg CO_3^-/L)	–	108
Chloride mg Cl^-/L)	–	8.0
Sulfate (mg SO_4^{-2}/L)	–	48
Nitrate (mg NO_3^-/L)	–	2.7

rich medium, Luria-Bertani (LB) broth, and incubated in a shaker incubator at 37 °C and 180 rpm. After 8 h, cells were diluted (1%, v/v) in the pre-heated LB broth and incubated at 37 °C for 15 h in the incubator until a stationary physiological phase was reached. Cells were separated during the stationary growth phase by centrifugation (15 min at 5000 rpm, at 4 °C). The bacterial pellet was re-suspended and washed for 10 min in the centrifuge (twice). This procedure resulted in a bacterial pellet of approximately 10^9 colony forming units per millilitre (CFU/mL).

2.3. Photocatalytic semiconductor and (photo)-Fenton-mediated inactivation experiments

All bacterial inactivation experiments were performed in Pyrex reactors (4 cm × 9 cm, 100 mL). The Pyrex reactors containing the bacterial suspension in Milli-Q water (approximately 10^6 CFU/mL) were placed in the dark at 25 °C under magnetic stirring for at least 30 min to let the bacteria adapt to the new matrix and to allow the die-off and equilibration of the most stress-sensitive species. In the experiments with cationic iron, $FeSO_4$ (0.6 mg/L of Fe^{2+}) were added to a solution of *E. coli*. Then, the pH was adjusted to 6.5 or 7.5 depending of the experiment and the samples were exposed to H_2O_2 (10 mg/L) and/or simulated solar light over 2 h, under continuous stirring. Aliquots were taken during set intervals within the inactivation time. These concentrations were determined experimentally as being optimal (results not shown) and corresponded to the limit, where bacterial inactivation could not be further enhanced, when more of Fe^{2+} was added [6].

In the experiments with iron (hydr)oxide particles, 0.6 mg/L of iron were added to a solution of *E. coli*. Then, the pH was adjusted to 6.5 and *E. coli* inactivation was studied for each particle type to test four different inactivation mechanisms: in the dark in Milli-Q water only (control), in the dark with H_2O_2 (dark Fenton), under sunlight (photocatalysis) and under sunlight, in the presence of H_2O_2 (photo-Fenton). H_2O_2 was added to the reactor as the last component at a concentration of 10 mg/L.

Photo-Fenton and photocatalysis experiments were carried out using a solar simulator CPS Suntest System (Heraeus Noblelight, Hanau, Germany). This solar simulator was equipped with a basic uncoated quartz glass light tube, a filter E and an IR screen (simulation of solar global radiation outdoors daylight). The irradiance was measured by a spectroradiometer, Model ILT-900-R (International Light Technologies) and corresponded to 820 W/m^2 of light global intensity (39 W/m^2 on the UV-A range).

During the experiments, the temperature in the reactors did not exceed 38 °C. After each experiment, the reactors were rinsed with nitric acid (10%) followed by an extensive water wash and finally autoclaved. All experiments were conducted in triplicate, with good reproducibility (<10% difference between replicates).

Bacterial reactivation and/or growth of bacteria was determined for some experiments by leaving the last samples in the dark at room temperature (20–25 °C) for 24 h before the measurement of the CFU.

2.4. Analytical methods

Dissolved Fe^{2+} was measured using the Ferrozine method as described previously [6] and total dissolved iron was measured using an Inductively Coupled Plasma Mass Spectrometer (ICP-MS), Model ICPE-9000 (Shimadzu, Japan). Samples were filtered (0.25 μm) and kept in acid solution prior to the determination. The detection limit ranges of spectrometry used for this experiment were (0.2–0.9 μg/L). The concentration of H_2O_2 was monitored using a titanium (IV) oxysulfate solution *via* a spectrophotometric method at 410 nm (modified method DIN 38 402 H15). The titanium (IV) oxysulfate method has a 0.1 mg/L detection limit. The bonding structure in particle samples was analyzed by Fourier transform infrared spectroscopy (Nicolet 6700 FT-IR), using the KBr self-supported pellet technique in the frequency range of 400–4000 cm^{-1}. The pH was measured with a pH-metre Metrohm 827 pH-lab using a glass electrode.

2.4.1. Electron spin resonance spectroscopy (ESR)

Electron spin resonance spectroscopy (ESR) in combination with spin-trapping were used to monitor the formation of ROS, namely hydroxyl ($^{\bullet}OH$) and superoxide ($O_2^{\bullet -}$) radicals, generated by photocatalytic semiconductor and heterogeneous photo-Fenton processes in the presence of iron (hydr)oxide. A stock solution of DMPO (0.5 M) was prepared in ultrapure water (Milli-Q) and was stored at −20 °C. Just before performing the photo-generation of ROS, DMPO (final concentration of 100 mM) was added to aqueous suspensions containing reagents. Subsequently, 2 mL aliquots of the prepared samples were transferred into small Pyrex beakers (5 mL volume, 20 mm outer diameter and 30 mm height) and exposed to simulated solar light (intensity 820 W/m^2) under constant agitation. Subsequently, the sample of the Fenton's reagents was drawn into thin glass capillaries (0.7 mm ID/0.87 mm OD, from VitroCom, NJ, USA), which were then sealed on both ends using the Cha-Seal^{TM} tube-sealing compound (Medex International, Inc. USA). ESR measurements were carried out at room temperature using a Bruker X-band spectrometer, Model EleXsys 500 (Bruker BioSpin, Karlsruhe, Germany) equipped with a high-Q cylindrical TE_{011} microwave cavity, Model ER4123SHQE. The typical instrumental settings were: frequency of 9.4 GHz; microwave power of 0.63 mW; scan width of 120 G; magnetic field resolution of 2048 points; modulation frequency of 100 kHz; modulation amplitude of 1.0 G; receiver gain of 60 dB; conversion time of 40.96 ms; time constant of 20.48 ms and sweep time of 84 s.

The spin-adducts concentrations were estimated using the double integration of the first-derivative ESR spectra. The actual concentrations of spin-adducts were derived by comparison with a calibrated ESR signal, which was acquired for a stable nitroxide radical, TEMPOL (10 μmol/L). The data analysis was carried out using Origin Pro 9.0 software.

3. Result and discussion

3.1. Photo-inactivation of bacteria in water by addition of $FeSO_4$ at pH 6.5 and 7.5 in the absence or presence of H_2O_2. Evolution of soluble forms of iron during the treatment

The Fig. 1 shows the complete *E. coli* inactivation under 90 min during the $FeSO_4$-based photo-Fenton treatment at initial pH 6.5 and 7.5 (Fig. 1, traces (▲) and (♦)). In particular, the photo-Fenton treatment at pH 6.5 showed faster bacterial inactivation rate (under 60 min), as compared with the same system at pH 7.5. This is due to the presence of dissolved ferrous iron ions in the system at pH 6.5 (Table 3). They contribute to the homogenous photo-catalytic cycle, thus accelerating the decomposition of H_2O_2, which, in turn, results in enhancement of $^{\bullet}OH$ production. This observation was corroborated by the hydrogen peroxide consumption that was greater for the photo-Fenton treatment at pH 6.5 than at pH 7.5 (Table 3).

The inactivation of *E. coli* by homogenous photo-Fenton process may be explained by several mechanisms. One possibility is an internal process, where endogenous photo-sensitizers and internal iron sources synergistically coupled with external UV and Fenton reactants lead to oxidative stress through the intracellular Fenton's reaction. As a result, highly toxic $^{\bullet}OH$ radicals are generated, which can directly attack DNA and other internal cell components, thus leading to bacterial growth inhibition. The other scenario might be due to the contribution of external pathways, where exogenous

Table 3
Values of pH, total dissolved iron (Fe^{tot} mg/L) and H_2O_2 during bacterial inactivation for different systems. Iron sulfate or iron (hydr)oxide: 0.6 mg/L, H_2O_2: 10 mg/L, irradiated with simulated solar light.

Iron(hydr)-oxide particles	pH		Fe (mg/L)			H_2O_2 (mg/L)		
	0 min	120 min	0 min	60 min	120 min	0 min	60 min	120 min
Fig. 1								
Iron sulfate + H_2O_2 + light	7.5	6.8	N.D.	N.D.	N.D.	10.0	8.0	7.4
Iron sulfate + light	7.5	7.1	N.D.	N.D.	N.D.	–	–	–
Iron sulfate + H_2O_2 + light	6.5	6.0	0.3	0.2	N.D.	10.0	5.2	5.0
Iron sulfate + light	6.5	6.2	0.4	0.3	0.1	–	–	–
Fig. 4a–d								
Wustite + H_2O_2 + light	6.5	6.3	N.D.	N.D.	N.D.	10.0	9.4	8.6
Wustite + light	6.5	6.2	N.D.	N.D.	N.D.	–	–	–
Hematite + H_2O_2 + light	6.5	6.3	N.D.	N.D.	N.D.	10.0	9.6	8.9
Hematite + light	6.5	5.9	N.D.	N.D.	N.D.	–	–	–
Magnetite + H_2O_2 + light	6.5	6.4	N.D.	N.D.	N.D.	10.0	9.3	9.3
Magnetite + light	6.5	6.3	N.D.	N.D.	N.D.	–	–	–
Goethite + H_2O_2 + light	6.5	6.2	N.D.	N.D.	N.D.	10.0	9.6	8.8
Goethite + light	6.5	6.3	N.D.	N.D.	N.D.	–	–	–

Experiments were conducted in triplicated and standard error was found to be approximately 5%. N.D.: not detectable.

ROS, such as singlet oxygen ($^1O_2$), H_2O_2 and •OH, are formed outside of the cell and can direct attack to the external cell membrane, thus initiating chain reactions of lipid peroxidation. This results in an increase of cell membrane permeability, impairs cellular functioning and severely affects cell viability [30]. In our opinion, the internal (photo)Fenton mechanism represents a key contribution to the overall inactivation process. This is based on our previous findings pointing to only very weak lipid peroxidation and slight cell permeability changes under photo-Fenton treatment at near-neutral pH [7].

In contrast to the same treatment at pH 6.5, dissolved iron was not detected in the filtrate samples during the reaction at pH 7.5 (Table 3). In the latter case, *E. coli* inactivation was achieved before 90 min of treatment (Fig. 1, trace (♦)), and was principally mediated by heterogeneous photo-Fenton reactions. Goethite (α-FeO(OH)) and/or lepidocrocite (γ-FeO(OH)) which have been reported to be formed by oxidation of Fe^{2+} in solution at neutral pH [31], are probably involved in this process.

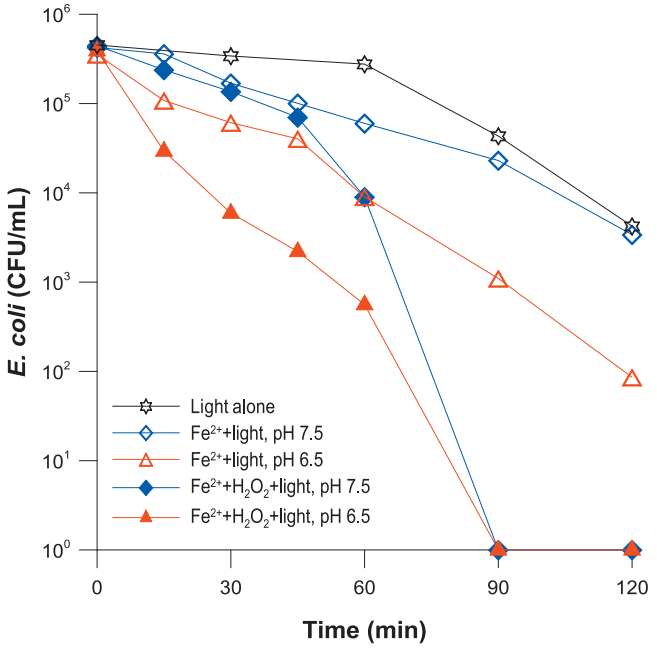

Fig. 1. *E. coli* inactivation by: (▲) photo-Fenton at pH 6.5; (♦) photo-Fenton at pH 7.5; (△) Fe^{2+}, under light at pH 6.5; (◊) Fe^{2+}, under light at pH 7.5; (☆) light alone. $FeSO_4$: 0.6 mg/L, H_2O_2: 10 mg/L. Experiments were conducted under simulated solar light and performed in triplicate (the standard error was found to be of ~5%).

In control experiments conducted in the absence of H_2O_2, for the Fe^{2+}/light system at pH 6.5, ~3.5 $\log_{10}$ reduction of the number of live bacteria was reached before 120 min of treatment (Fig. 1, trace (△)). As can be seen in Table 3, dissolved iron was present throughout treatment. The bactericidal effect of the photo-assisted Fe^{2+} is the result of the combined action of the Fe^{2+} and light into the bacterial cell. Indeed, added Fe^{2+} can easily diffuse into the cell [7,32] and catalase, which regulates H_2O_2 concentration into the bacteria, is degraded by UVA radiation, leading to intracellular Fenton reactions enhancement. On the contrary, in the experiments conducted at pH 7.5, Fe^{2+} was effectively oxidized and transformed in solid iron forms by O_2, in the absence of H_2O_2 (Table 3). This system was not efficient neither as heterogeneous photocatalyst nor as semiconductor, as it lead only to ~2 $\log_{10}$ reduction of bacteria in 120 min of treatment values similar to the bacterial inactivation reached under a light-alone system (Fig. 1, traces (◊) and (☆)). The solid iron formed at pH 7.5 does not enhance significantly the photo-inactivation of bacteria, probably because this pH is close to the isoelectric point of goethite (IEP = 7.5–8.5) and lepidocrocite (IEP = 7.3–7.5) which are iron oxides formed by oxidation of Fe^{2+} at this pH [21]. Thus, the contact/attraction of >FeOH groups with average negative membrane of *E. coli* is not favourable because hydroxyl groups at the iron oxide surface are uncharged.

The effect of the presence of bacteria in the solubilization of iron during photo-Fenton process was evaluated at pH 6.5 and 7.5. Table 4 shows that soluble iron species were not detected during the $FeSO_4$-based photo-Fenton system at pH 6.5 and 7.5 in the absence of bacteria. It was the result of the formation of the aquo hydroxo zero-charge complexes, which are the precursors of the solid-phase iron [12], formed in the absence of complexing ligands. On the contrary, in presence of bacteria, complexing substances are liberated from the beginning or generated as by-products during bacterial inactivation. This explains why soluble iron was detected at pH 6.5 when bacteria are present. It could be mediated by secreted siderophores (*e.g.* ferritins and aerobactin from *E. coli*) [33] that can chelate iron, allowing its solubilization. The photo-reduction of Fe^{3+}-siderophore complexes under UVA and visible radiation, produces •OH and regenerates Fe^{2+} *via* ligand-to-metal charge transfer (LMCT) [34,35]. In contrast to pH 6.5, at pH 7.5 no dissolved iron was observed in presence of bacteria during entire treatment period even if detection limit ranges of ICP-MS spectrometry used for this experiment were 0.2–0.9 μg/L. This could be due to the crystalline non soluble forms of iron species formed at high pH (7.5), which are more stables

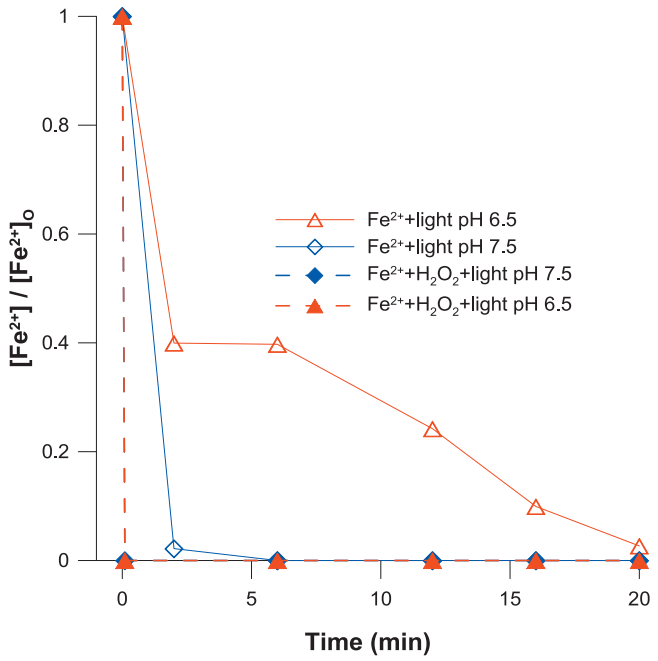

Fig. 2. The time evolution of the ferrous iron ions concentration remaining in solution at pH 6.5 (◊) and 7.5 (Δ), in the presence (- - -) or absence (—) of 10 mg/L H_2O_2. $[Fe^{2+}]_o$ = 0.6 mg/L. Experiment performed in absence of bacteria. Experiments were conducted under simulated solar light and performed in triplicate (the standard error was found to be of ~5%).

to be photo-reduced by siderophores [36]. These results are in concordance with those reported by Waite and Morel [37], who detected photo-reduced iron from amorphous Fe-hydroxides at pH 6.5, but not at pH 8.0. They proposed that a hydroxylated ferric surface species is the primary chromophore (light absorbing compound), analogous to the photoreduction of $Fe(OH)^{2+}$, and that at pH 8 the Fe^{3+} surface complex was more strongly hydrolyzed and less prone to photoreduction.

3.1.1. Identification of generated solid species in the $FeSO_4$-based photo-Fenton process in the absence of bacteria at pH 6.5 and 7.5

Fig. 2 shows the decrease in dissolved Fe^{2+} concentration in a stirred water solution, initiated with 0.6 mg/L of Fe^{2+} (as $FeSO_4$) at pH 6.5 and 7.5. It was conducted in the absence of bacteria and in the absence or presence of H_2O_2 (10 mg/L). In the absence of H_2O_2, a remarkable difference in Fe^{2+} oxidation rates and subsequent precipitation of generated iron oxides were observed at pH 6.5 and 7.5 (Fig. 2, traces (—Δ—) and (—◊—)). The loss of ferrous ions in the solution in the absence of H_2O_2 is due to the oxidation by dissolved oxygen. Morgan and Lahav reported that at neutral pH and $[Fe^{2+}]$ <1 mg/L, soluble iron species like $[Fe]^{2+}$, $[Fe(OH)]^{+}$ and $[Fe(OH)_2]$ are initially formed in the aqueous system, according to Eqs. (8)–(10) before undergoing subsequent oxidation by O_2 (Eqs. (11)–(13)). However, "hydrolysed" ferrous iron species are more readily oxidized than non-hydrolysed ones in the following order: $[Fe(OH)_2] \gg [Fe(OH)]^{+} \gg [Fe]^{2+}$ [11]. The oxidation of soluble ferrous species $[Fe(OH)_2]$ by O_2 (Eq. (13)), producing partially oxidized ferro-compounds like meta-stable ferrous–ferric species as $[Fe_4(OH)_8(H_2O)_8]$ (Eq. (14)). These compounds are subsequently transformed into end-products such as hematite, magnetite, goethite, and lepidocrocite, which are insoluble ferric species (Eq. (15)) [12].

The fact that dissolved Fe^{2+} was not found shortly after the addition of H_2O_2, confirms the loss of ferrous ions in the solution at both pH levels (Fig. 2, traces (-- ▲ --) and (-- ◆ --)). Thus, the addition of H_2O_2 increases oxidation rates, indicating that both O_2 and H_2O_2 contribute to the fast oxidation of ferrous iron species at neutral pH and, in concert, lead to spontaneous oxidation and subsequent formation of insoluble ferric species. Therefore, in the absence of complexing ligands (secreted by bacteria from the beginning or generated as by-products during bacterial inactivation), soluble iron species are negligible in a photo-Fenton process at neutral pH,

$$Fe^{2+} + 6H_2O \rightarrow [Fe(H_2O)_6]^{2+}{}_{(aq)} \quad (8)$$

$$[Fe(H_2O)_6]^{2+}{}_{(aq)} + OH^- \rightarrow [Fe(OH)(H_2O)_5]^{+}{}_{(aq)} \quad (9)$$

$$[Fe(OH)(H_2O)_5]^{+}{}_{(aq)} + OH^- \rightarrow [Fe(OH)_2(H_2O)_4]_{(aq)} \quad (10)$$

$$Fe^{2+} + O_2 \rightarrow Fe^{3+} + O_2^{\bullet -} \quad (11)$$

$$Fe(OH)^{+} + O_2 \rightarrow Fe(OH)^{2+} + O_2^{\bullet -} \quad (12)$$

$$Fe(OH)_2 + O_2 \rightarrow [Fe(OH)_2]^{+} + O_2^{\bullet -} \quad (13)$$

$$4[Fe(OH)_2(H_2O)_4]_{(aq)} \rightarrow [Fe_4(OH)_8(H_2O)_8]_{(S)} + 8H_2O \quad (14)$$

$$[Fe_4(OH)_8(H_2O)_8]_{(S)} + O_2 \rightarrow 4FeOOH_{(S)} + 10H_2O \quad (15)$$

To identify the solid iron species formed during the photo-Fenton treatment at pH 6.5 and 7.5 in the absence of bacteria, the precipitated iron were recovered for FT-IR analysis. Although the sample colour was yellow for insoluble iron species obtained at pH 6.5 and brown for these obtained at pH 7.5, the IR spectrum was similar for both compounds. This could be due to the variation of parameters affecting the surface area and morphologies of the precipitate as follows: the final pH of the solution, which specially influences the Fe:OH ratio, the precipitation rate (slow/fast), temperature (usually 40–90 °C) and the time of hydrolysis and oxidation process (minutes to weeks) [12]. In our case, the last three parameters were well controlled and, consequently, only the Fe:OH ratio, related to the final pH of the solution, affected the colour of the samples.

Fig. 3 shows the infrared spectra of insoluble ferric species obtained at pH 7.5. The three absorption band observed at approximately 740, 553 and 462 cm^{-1} correspond to those of α-FeOOH, which can be attributed to the stretching vibration of Fe—O and Fe—O—H [38]. The band at 553 cm^{-1} is assigned to the hexagonal environmental characteristic of hematite or goethite [39]. The band at 491 cm^{-1} confirms the octahedral positions of the H_2O and OH groups in the ferric complexes [38,40]. The absorption band above 3000 cm^{-1} is originated by the H-bonded OH groups, since the isolated OH groups absorb above 3600 cm^{-1}. This broad peak is due to the combined contributions of iron (hydr)oxide, and the adsorbed water in the samples. Iron hydroxide, if present, may also contribute to this broad peak. Absorption bands at 3396 and 1633 cm^{-1} are characteristic bending vibration of O—H of crystal water, indicated the presence of water in the coordination sphere of the metal.

Table 4
Values of total dissolved iron (Fe^{tot} mg/L) from $FeSO_4$-based photo-Fenton processes in presence and absence of bacteria. $FeSO_4$: 0.6 mg/L, H_2O_2: 10 mg/L, irradiated with simulated solar light.

Initial pH	Time	Dissolved iron (mg/L) in absence of *E. coli*	Dissolved iron (mg/L) in presence of *E. coli*
6.5	0	N.D.	0.4
	15	N.D.	0.4
	30	N.D.	0.4
	60	N.D.	0.2
	120	N.D.	N.D.
7.5	0	N.D.	N.D.
	15	N.D.	N.D.
	30	N.D.	N.D.
	60	N.D.	N.D.
	120	N.D.	N.D.

Experiments were conducted in triplicated and standard error was found to be approximately 5%. N.D.: not detectable.

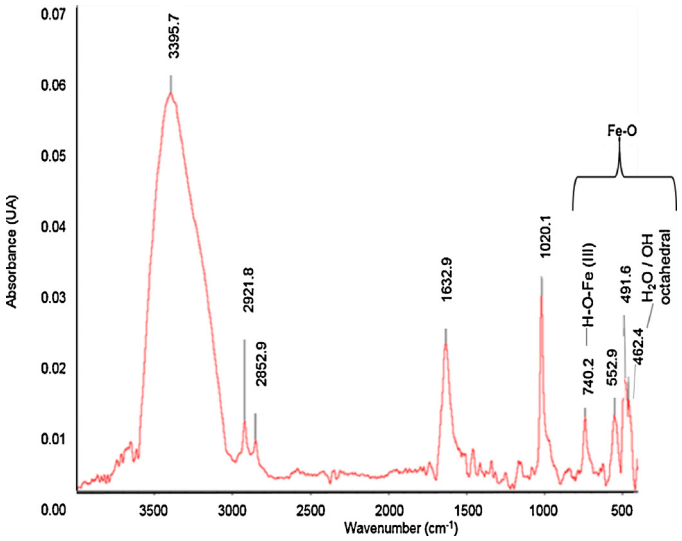

Fig. 3. FT-IR spectra of ferric precipitates formed during the photo-Fenton reactions at pH 7.5.

Furthermore, the absorption band at 1020 cm^{-1} is produced by HO—Fe interaction in the (0 1 0) plane bending of lepidocrocite (γ-FeOOH) [41]. Considering all these features, the observation of the infrared spectra in Fig. 3 leads to the conclusion that the insoluble iron species formed under photo-Fenton process at pH 6.5 and 7.5 are mainly iron (hydr)oxide alone or mixed as goethite (α-FeOOH) and lepidocrocite (γ-FeOOH).

3.2. Contribution of photocatalytic semiconductor vs heterogeneous photo-Fenton processes to bacterial inactivation at neutral pH

In our previous work [7], we have demonstrated that goethite was beneficial for bacterial inactivation at near-neutral pH, both as a photocatalytic semiconductor and as heterogeneous photo-Fenton catalyst. To determine whether iron (hydr)oxide enhanced inactivation, and to determine whether such an enhancement is due to photocatalytic semiconducting mechanism or heterogeneous photo-Fenton reactions, bacterial inactivation studies were conducted in the presence of different commercial iron (hydr)oxides, as well as H_2O_2 and/or simulated solar light. The iron (hydr)oxide compounds selected were: goethite and hematite because these are the most reactive and abundant solid iron oxides present in nature (sources of iron Fe^{3+}) [21], magnetite (source of iron Fe^{2+}/Fe^{3+}), and wüstite (source of iron Fe^{2+}) which exists also in nature [42]. Fig. 4(a–d) shows that in the dark, the studied iron (hydr)oxides did not yield inactivation in the absence or presence of H_2O_2, indicating that heterogeneous Fenton processes (iron (hydr)oxides and H_2O_2) did not contributed to bacterial inactivation under our experimental conditions. These results are in contradiction with some studies, dealing with magnetite as Fenton catalyst, and reporting that it is a promising catalyst for oxidative processes for dye removal, and phenol and aromatic hydrocarbon degradation at acid pH [14,43]. They explained that magnetite has a combination of +2 iron and +3 iron atomic states that aids to increase decomposition of hydrogen peroxide and the production of •OH that enhance decomposition of organic contaminants. This was not observed in our experiments on bacterial inactivation (Fig. 4d) possibly due to:

(i) The uncharged magnetite surfaces in our experimental pH of 6.5 (IEP: 6.0–6.5 (Table 1)) offer unfavourable sites for the adsorption of negatively charged bacteria. It was reported that adsorption onto magnetite particles was a prerequisite for achieving significant virus inactivation [27],

(ii) The formation of the particle agglomeration that was favoured in our experimental conditions (pH 6.5, Table 3) since agglomeration is enhanced when pH values of the suspension is near to isoelectric point of the material [44,45]. Agglomeration of magnetite particles affects the available reactive surface area (site blockage) as the active sites can become less accessible for bacteria and for H_2O_2 (kinetic effect) [46]. This can explain the lower consumption of H_2O_2 during magnetite-based photo-Fenton systems compared to the other iron (hydr)oxides that contain only Fe^{3+} in the structure, as goethite and hematite (data not shown),

(iii) The oxidation of structural Fe^{2+} to Fe^{3+} by O_2 and H_2O_2. This oxidation produces an outer Fe^{3+} oxide layer which reduces electron transfer activity on the surface and inhibits the catalytic efficiency towards Fenton catalysis [47,48]. Kong et al. [49] compared to surface of unused magnetite, that of used magnetite treated with H_2O_2. Used magnetite exhibited self-precipitate as revealed by scanning electron microscopy (SEM) analysis. This precipitate seemed to cause lower treatment efficiency in magnetite system.

Wüstite (FeO) also contains Fe^{2+} in the structure but its efficiency in Fenton processes for bacterial inactivation was also very low probably because of the same reason (the oxidation of structural Fe^{2+} to Fe^{3+} by O_2 and H_2O_2) that that proposed for magnetite. The use of wüstite as heterogeneous Fenton catalysts is not documented in the literature.

The combination of iron (hydr)oxides and light show semiconductor properties with a narrow band gap of 2.2 eV for hematite, 2.1 eV for goethite, and 2.4 for wüstite (Table 1). Photo-inactivation curves with goethite and hematite showed a shoulder (Fig. 4a and b). This initial period of latency indicates that a contact between bacteria and oxide was necessary and that self-defence mechanisms of bacteria have to be overpassed to effectively photo-inactivate bacteria with these oxides. After that, the bacterial inactivation rate increased considerably. Thus, goethite, hematite and wüstite were photoactive under simulated solar light irradiation to efficiently inactivate bacteria, using only oxygen (from air) as electron acceptor. Similarly, in our previous work, we have demonstrated the photocatalytic semiconducting activity of goethite towards bacterial inactivation [7]. In contrast, magnetite was not capable of inactivating bacteria under light (Fig. 4d, trace (Δ) and its negative screen effect was observed with regard to the control experiment under light alone (Fig. 4d trace (☆)). This is the result of the narrower band gap of the magnetite (0.1 eV) compared to those of goethite, hematite and wüstite (2.2–2.4 eV) (Table 1) and the existence of both Fe^{2+} and Fe^{3+} in its lattice, leading to a continuous electron hopping between the two, which increases the electron–hole recombination and the lowering of its photoactivity [21,50–52]. Furthermore, the extent of recombination depends to some extent on the pH of the solution and its effect on the proportion of >FeOH groups at the surface [23]. Thus, as was mentioned before, the contact/attraction of >FeOH groups with *E. coli* is not favourable because hydroxyl groups at the surface are uncharged, leading to an increase in the electron–hole recombination rate [23] and a decrease in the efficiency of the reactions of the valance-band hole with bacteria. In addition, the photo-generated holes in the valence-band of magnetite have weak oxidation potential which is not enough to generated •OH. Goethite and hematite present an IEP between 7.5 and 8.5 (Table 1) [21], indicating that hydroxyl groups at the surface are partially protonated (>Fe—OH_2^+). The surface interaction of >Fe—OH_2^+ with *E. coli* is favoured by electrostatic attraction forces because the *E. coli* surface is negative

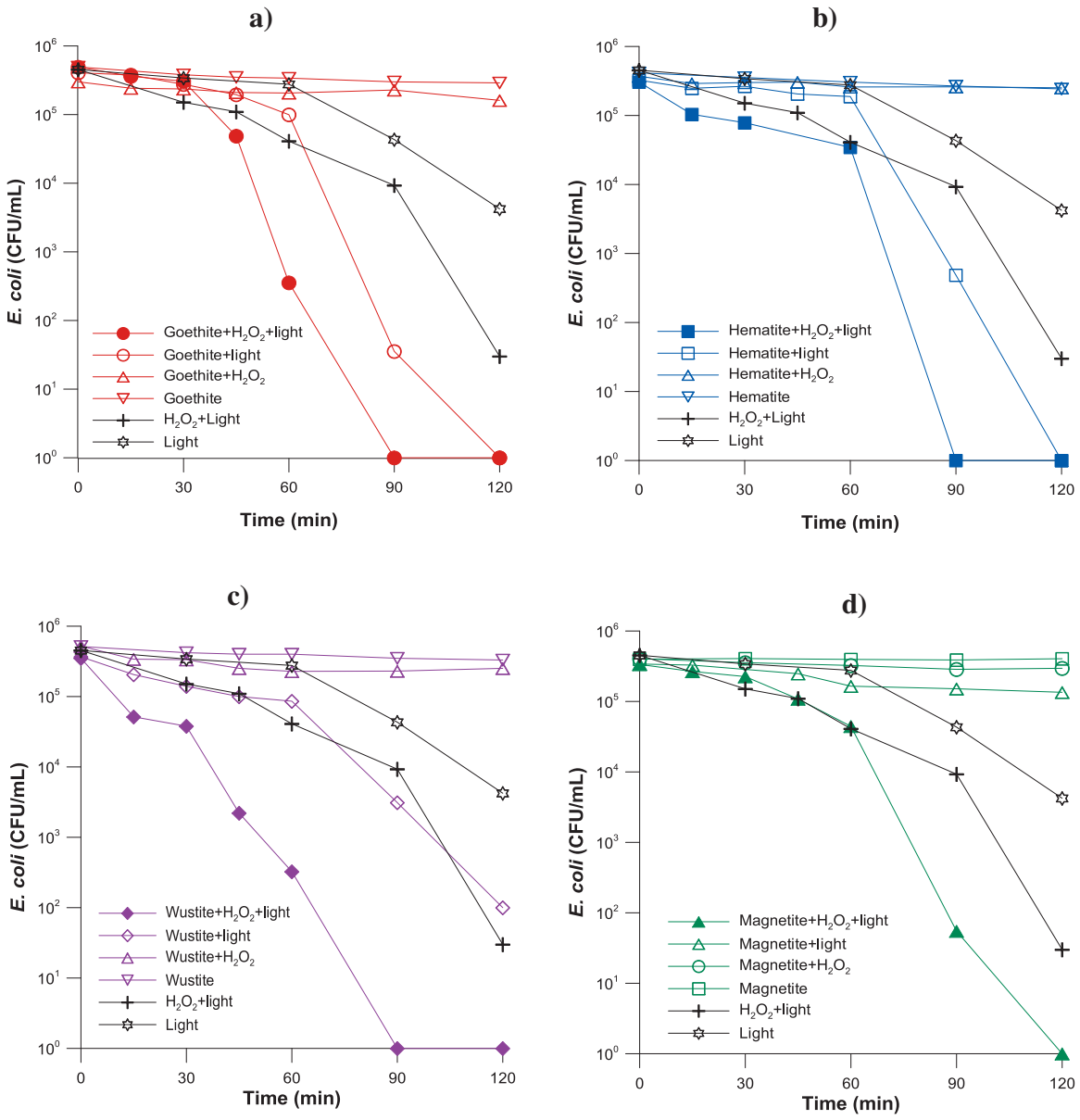

Fig. 4. *E. coli* inactivation by iron (hydr)oxide particles in the presence or absence of sunlight and H_2O_2 for (a) goethite, (b) hematite, (c) wüstite and (d) magnetite. Experimental conditions: pH 6.5 and concentrations of iron (hydr)oxides and H_2O_2, 0.6 mg/L and 10 mg/L, respectively. Experiments were conducted under simulated solar light and performed in triplicate (the standard error was found to be of ~5%).

charged between pH 3 and pH 9 due to the phospholipids and lipopolysaccharides on its cell surface [53].

The iron hydr(oxides) particles studied under the simultaneous presence of light and H_2O_2 caused considerable bacterial inactivation enhancement when compared with the other systems and with control experiments (Fig. 4a–d). *E. coli* inactivation was reached before 90 min of treatment for goethite, hematite and wüstite (Fig. 4a–c) and at 120 min for magnetite (Fig. 4d). The total dissolved iron was determined by ICP-MS spectrometry during the reaction process. Photo-dissolution of iron hydr(oxides) was not significant in the reactions since the concentration of total iron was below detection limit. Thus, *E. coli* inactivation with iron hydr(oxides) was in this case mediated principally by a heterogeneous (photo)-Fenton process. Such systems combine photocatalytic semiconductor character and photo-assisted heterogeneous Fenton oxidation in a single material.

Even if dissolved iron was not detected, during the iron (hydr)oxide-based photo-Fenton treatment (Table 3) due to a fast reoxidation of surface Fe^{2+} in the presence of O_2 and H_2O_2 at neutral pH, probably a small contribution of homogenous photo-Fenton process have to be considered in bacterial inactivation, resulting from photo-dissolution of iron (hydr)oxide promoted by siderophores. Siderophores secreted by many bacteria, have shown to significantly increase the light-induced dissolution of goethite and other iron (hydr)oxides [33,34,54]. The effect of siderophores in the light-induced redox cycling of dissolved iron is dominated by photo-reduction of certain Fe^{3+}-siderophore complexes resulting in the formation of Fe^{2+}. According to Borer et al. [54], the possible mechanisms of Fe^{3+} photo-reduction at the iron oxide surface in the presence of siderophores are: (i) photolysis of Fe^{3+}-siderophore complexes leads to the formation of Fe^{2+} or (ii) semiconductor charge transfer mechanism with subsequent migration of the generated photoelectron to the oxide surface. Absence of detection of dissolved iron in the bulk of the solution could be related with the low concentration of iron (hydr)oxides used in the treatments. Indeed, the degree of dissolution is principally dependent on the

iron (hydr)oxides concentration and is highest at lower pH and at high colloidal surface area [37]. No bacterial reactivation and/or growth was observed after 24 h and 48 h of dark storage for the iron (hydr)oxide-based photo-Fenton treatment. The same antimicrobial activity was obtained for the photocatalytic semiconducting action of hematite and goethite. Additionally, a delayed disinfection effect was observed to continue in the dark for the photo-assisted wüstite-based treatment.

The relative little difference of required time to inactivate bacteria by photo-assisted hematite and goethite in the presence (90 min) or absence (120 min) of H_2O_2 suggest that from the application point of view, small concentrations (0.6 mg/L) of these iron (hydr)oxides can be applied as semiconductor to efficiently disinfect water. These results are interesting because the omission of H_2O_2, significantly reduces the cost of the treatment. Therefore, the iron (hydr)oxide particles, including those already present in environmental waters, have great potential for low-cost "photocatalyst" in solar water disinfection, as it has already been demonstrated in our previous work in Africa [55].

3.3. *ROS generated by photocatalytic semiconductor and heterogeneous photo-Fenton processes in the presence of iron (hydr)oxide*

In general, the ability of iron oxide particles to produce ROS under light defines their potential to inactivate microorganisms or degrade biomolecules by oxidation. Therefore, by employing the ESR spin-trapping technique, we identified and quantified ROS, *i.e.* $^{\bullet}OH$, $O_2^{\bullet-}$ and singlet oxygen ($^1O_2$), produced photo-assisted iron (hydr)oxide in the absence or presence of H_2O_2. DMPO was used as a spin trap to identify both $^{\bullet}OH$ and $O_2^{\bullet-}$ radicals, thus leading to the formation of spin-adducts, DMPO—OH or DMPO—OOH, respectively. Both resulting paramagnetic products reveal distinct and easily recognizable ESR spectra. However, the DMPO—OOH spin adduct is well known to be highly unstable and rapidly decomposes into the DMPO—OH spin adduct [56]. Therefore, as a result, a characteristic ESR spectrum of the DMPO—OH spin adduct consisting of four well resolved peaks (1:2:2:1 quartet, $a_N = a_H = 14.9$ G) was observed (insert in Fig. 5).

Fig. 5 (a and b) shows that ESR signals of DMPO—OH were not detected before illumination in the experiments. These results suggest that exposure to the simulated solar light was essential for generation of ROS for the iron (hydr)oxide in the absence or presence of H_2O_2. The growth of the ESR signal intensity of DMPO—OH confirmed the generation of $^{\bullet}OH$ and $O_2^{\bullet-}$ radicals, contributing in the photocatalytic semiconducting process of iron (hydr)oxide (Fig. 5a). A higher ESR signal intensity for photo-assisted hematite system was observed compared with goethite, even if the bacterial inactivation rate was similar (120 min) (Fig. 4a, b, traces ◯, □). It could be result of the different physico-chemical properties of the iron (hydr)oxides used as IEP, particle size, specific surface area of particle, *etc.* that influences in the ROS generation [57,58]. This result is in agreement with previous findings by Xu et al. [58], who reported that among the oxides, hematite is the most active in $^{\bullet}OH$ generation under neutral pH. Photo-assisted magnetite generated very low $^{\bullet}OH$ radicals production (Fig. 3a), that is in correlation with the negligible bacterial inactivation rate observed in Fig. 4d, trace △. Possibly due to the aggregation of magnetite particles, and the weak oxidative potential of the photo-generated holes in the valence-band as were explained before.

The mechanism of ROS generation by iron (hydr)oxides illuminated under simulated solar light involves semiconductor photocatalysis [21,58,59]. Thus, the photo-induced reactive species (electron–hole pairs) are formed on iron oxides under illumination (Eq. (1)). Conduction band electrons could react with O_2 to form superoxide radicals ($O_2^{\bullet-}$) [59] (Eq. (2)), followed by reaction

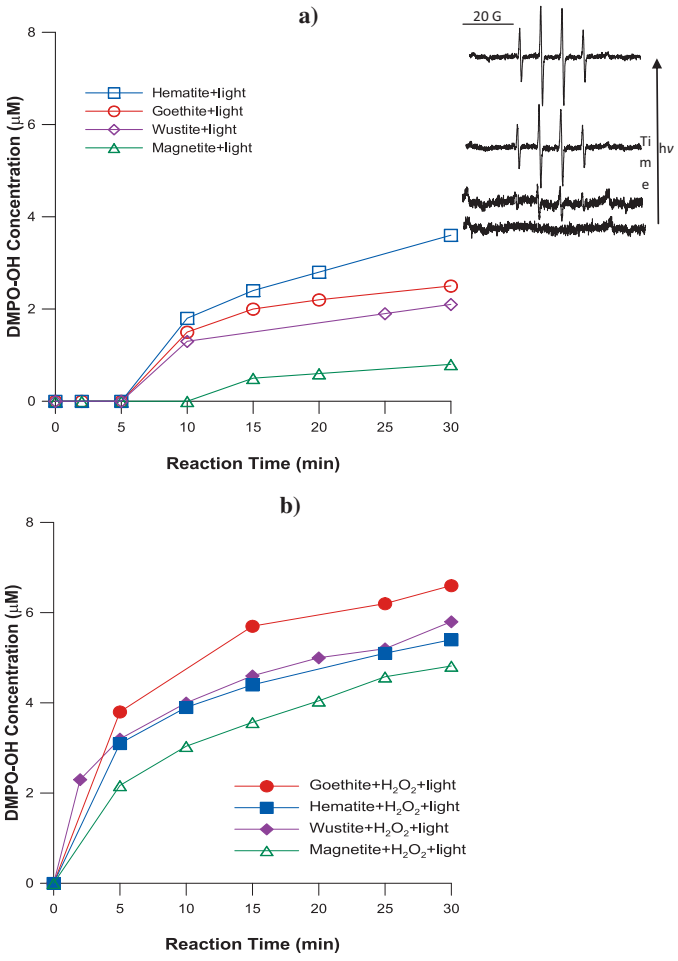

Fig. 5. The ESR-measured formation of hydroxyl radical in aqueous suspensions of iron (hydr)oxide particles under simulated solar light: (a) in the absence of H_2O_2 and (b) in the presence of 10 mg/L of H_2O_2. *Inset*: typical ESR traces of the paramagnetic spin adduct, DMPO–OH. Iron (hydr)oxide concentrations 3.8 mg/L, pH 6.5.

between hole and superoxide radical to form singlet oxygen as given by Eq. (3). Also electrons could participate in the regeneration of Fe^{2+} species (Eq. (4)). It was reported that the valence band (VB) of the iron (hydr)oxides is above the $OH^-/^{\bullet}OH$ potential [58]. Therefore, the oxidation of OH^- by holes in the iron (hydr)oxides VB is thermodynamically unfavoruable, leaving O_2 reduction as the most viable pathway for ROS production. On the contrary, holes in the excited surface of iron (hydr)oxides can directly react with bacteria (Eq. (5)). It is thermodynamically favourable because hole possess a positive oxidation potential of ~+1.7 at pH = 7 [58,60], that is below to the redox potential of microorganism and cell (redox potential of bacteria +0.45 to +0.72 V *vs.* SCE, pH = 7) [61–63].

Alternatively, Xu et al. [58] proposed that the formation of H_2O_2 and $^{\bullet}OH$ (Eqs. (16) and (17)) in photo-assisted hematite suspensions involved reduction of O_2 of electrons (Eq. (2)), which was inhibited under anaerobic conditions.

$$e^-_{(cb)} + O_2^{\bullet-} + 2H^+ \rightarrow H_2O_2 \quad (16)$$

$$e^-_{(cb)} + H_2O_2 \rightarrow OH^- + {}^{\bullet}OH \quad (17)$$

Nevertheless, some controversy exists in the literature about the photocatalytic properties of goethite and iron oxides particles. Kiwi et al. [64] argued that the semiconductor mechanism is not likely to be important except in very small (colloidal) iron oxide particles because of the short diffusion length of electrons and holes in iron oxide semiconductors.

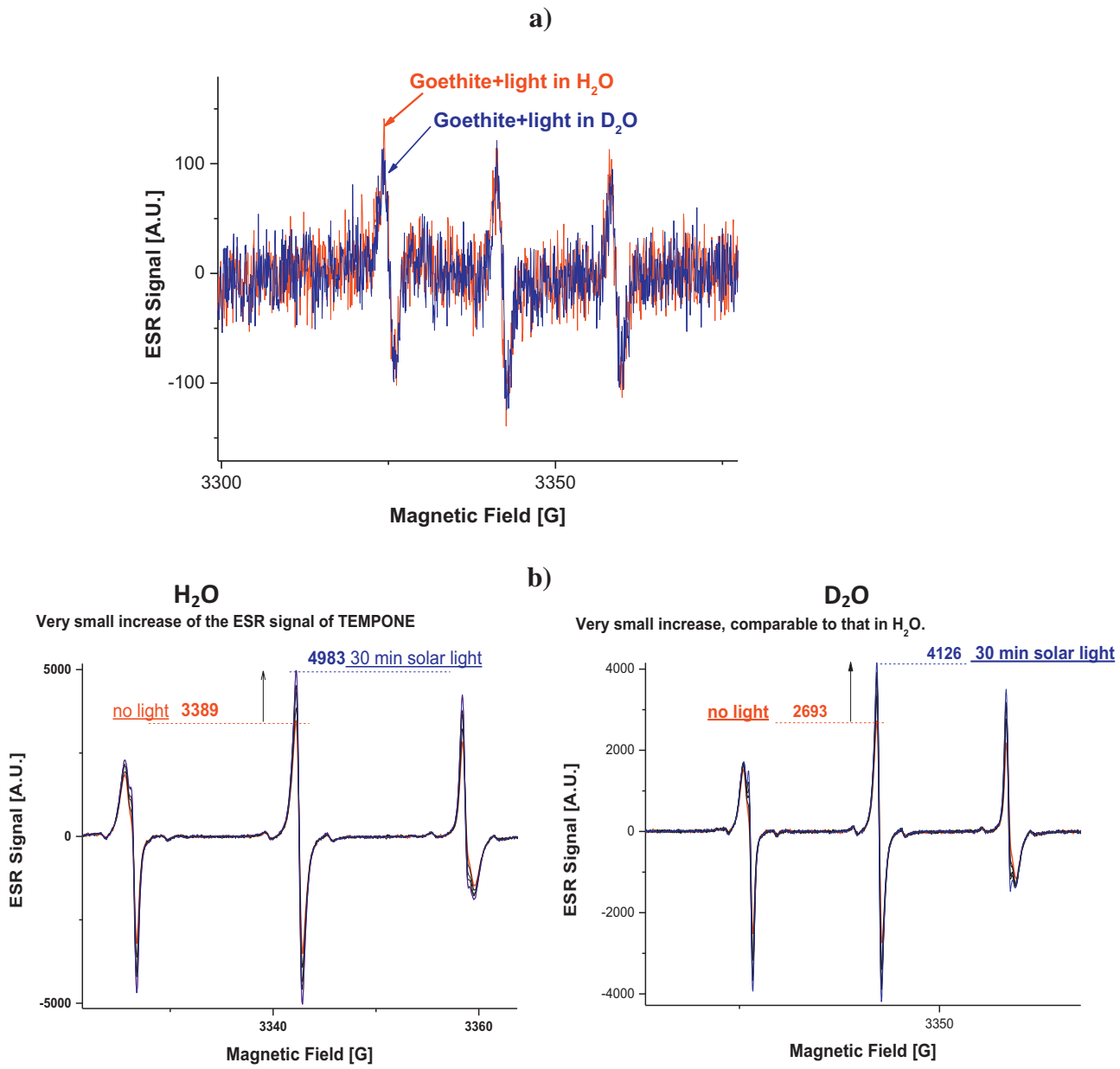

Fig. 6. (a) ESR spectra of TEMPOL photo-generated in the aqueous suspensions of goethite in the presence of singlet oxygen scavenger, TMP-OH, observed after 30 min of illumination by simulated solar light in H_2O (red trace) and D_2O (blue trace). Experimental conditions: concentrations of TMP-OH and goethite were 15 mM and 3.8 mg/L, respectively. (b) The time evolution of ESR spectra of TEMPONE photo-generated in the aqueous suspensions of goethite the presence of singlet oxygen scavenger, TEMPONE precursor (50 mM). Left: ESR traces recorded in H_2O. Right: ESR traces recorded in D_2O. Goethite concentration:15 mg/mL. (For interpretation of the references to colour in figure legend, the reader is referred to the web version of the article.)

The reactive ROS formed during these processes at the iron (hydr)oxide surface and the direct oxidation of bacteria by surface holes contributed to achieving complete bacterial inactivation for the goethite, hematite and ~3 $\log_{10}$ reduction of bacteria for the wüstite after 120 min of treatment under simulated solar light (Fig. 4a–c).

The presence of H_2O_2 in the photo-assisted iron (hydr)oxide suspension promoted a rapid generation of •OH (Fig. 5b), that contributed to a more efficient bacterial inactivation observed in Fig. 4 (a–d). The beneficial effect of the added H_2O_2 under light is due its electron acceptor properties. Thus, electrons generated on illuminated iron oxides from Eq. (1) are trapped by the H_2O_2 forming •OH (Eq. (17)). Also H_2O_2 initiates chain reactions by heterogeneous Fenton reactions (Eqs. (18) and (19)), leading to the formation of hydroperoxyl radical (HO_2•) by contact with Fe^{3+} sites available on the surface of iron particles dispersed in aqueous solution. Concomitantly, Fe^{3+} is reduced to Fe^{2+} (Eq. (18)). New Fe^{2+} reaction sites are then formed and allow H_2O_2 to generate •OH radicals when the Fe^{3+} sites are recovered through oxidation of Fe^{2+} in the cyclic mechanism (Eq. (19)). The Fe^{2+} regeneration (which is the rate determinant step of Fenton reaction) could occur *via* the photo-reduction of Fe^{3+} species (Eq. (6)) as well, through the photo-Fenton reaction (Eq. (20)).

$$>Fe^{3+} + H_2O_2 \rightarrow >Fe^{2+} + H^+ + HO_2\bullet \quad (18)$$

$$>Fe^{2+} + H_2O_2 \rightarrow >Fe^{3+} + OH^- + \bullet OH \quad (19)$$

$$>Fe^{3+} + H_2O_2 + h\nu \rightarrow >Fe^{2+} + H^+ + \bullet OH \quad (20)$$

He et al. [13] suggested a different reaction mechanism for the heterogeneous photo-Fenton reaction under UV-light irradiation in

the presence of hematite and goethite, based on the experimental observations of degradation of a model Azo dye, Mordant Yellow 10 (MY10):

$$>Fe^{3+}OH + H_2O_2 \rightarrow >Fe^{3+}OOH + H_2O \quad (21)$$

$$>Fe^{3+}OOH + h\nu \rightarrow >Fe^{4+}{=}O + {}^{\bullet}OH \quad (22)$$

$$>Fe^{4+}{=}O + H_2O \rightarrow >Fe^{3+}OH + {}^{\bullet}OH \quad (23)$$

The reactions are initiated by the formation of a precursor surface complex of H_2O_2 with the oxide surface metal centres. Under UV irradiation, the excited $>Fe^{3+}OOH$ bond is broken to produce $>Fe^{4+}{=}O$ species and $^{\bullet}OH$ radical. The $>Fe^{4+}{=}O$ is highly unstable and reacts immediately with H_2O forming another active hydroxyl radical. Therefore, the radicals photogenerated from Eqs. (17)–(23) increase the signal of DMPO—OH in Fig. 5b and contribute to enhance bacterial inactivation (Fig. 4a–d).

Previous studies have reported that in aqueous suspensions containing goethite under room light (wavelength between 400 and 700 nm) at pH 7.5 in the absence and presence of the H_2O_2, not $^{\bullet}OH$ radicals but singlet oxygen and superoxide ions acts as a keys reactive species of the ROS [59,65,66]. Nevertheless, in our experimental conditions (UV containing light), the DMPO—OH signal was generated in a significant extend (Fig. 5a and b, traces (○) and (●)), which were completely inhibited in the presence of $^{\bullet}OH$ scavenger, isopropyl. We also performed ESR reactive trapping experiments using TMP-OH as singlet oxygen scavenger. The formation of singlet oxygen was confirmed by observation of a characteristic 1:1:1 triplet signal of TEMPOL (Fig. 6a). However, no convincing 'isotope' effect was observed, when the standard Milli-Q water was replaced by heavy water (D_2O). This isotope effect, if present, could be associated with $^1O_2$ generation by photo-assisted goethite and hematite suspensions. Although a weak ESR signal of TEMPOL was detected, thus indicating that production $^1O_2$ for photo-assisted goethite and hematite in the absence or presence of H_2O_2 under simulated solar light is negligible. This result was confirmed using another precursor, TEMPONE, which monitors predominantly the formation of $^1O_2$ in the polar phase (Fig. 6b). Therefore, the principal radicals produced in our experimental conditions for the photo-assisted iron (hydr)oxide tested in the absence or presence of H_2O_2 were $^{\bullet}OH$ and $O_2^{\bullet-}$ radicals.

3.4. Bacterial inactivation in natural water by photocatalytic semiconducting and photo-Fenton action of hematite

In order to evaluate the effect of dissolved organic and mineral matter present in natural drinking water sources on the activity of hematite during bacterial inactivation, water coming from the Geneva Lake was used and was compared with Milli-Q water. Fig. 7 (traces (□) and (□)) shows complete *E. coli* inactivation before 120 min of treatment for hematite/light system in both, natural and Milli-Q water. Thus, the components of natural water (Table 2), did not inhibit the photocatalytic semiconducting action of hematite against bacterial inactivation in a significant extent. It was reported that under UV radiation, dissolved organic matter (DOM) can be involved in positive mechanics to contribute to inactivation of bacterial by the action of photo-sensitizer species [67]. Here the excited triple state ($^3DOM^*$) promoted by UV light absorption by DOM has not shown a significant contribution. However, the chemical components of the natural water enhance the bacterial inactivation by heterogeneous photo-Fenton action of hematite. As showed in Fig. 7 (trace (■)), at 60 min of treatment, 3 $\log_{10}$ of bacteria were inactivated in lake water compared with less than 1 $\log_{10}$ in Milli-Q water (Fig. 7, trace (■)) respectively. This is related with the presence of natural organic matter (NOM) which has a positive effect on the complexation and solubilization of iron, that concomitantly participates in homogenous photo-Fenton reaction generating additional

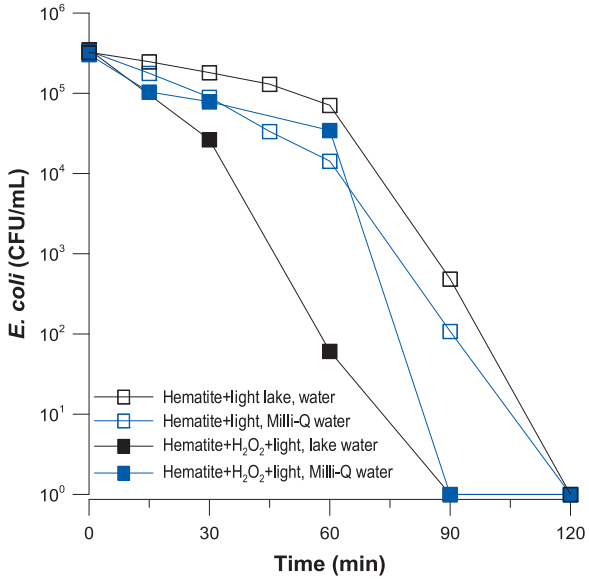

Fig. 7. *E. coli* inactivation by photo-assisted hematite in the presence and absence of H_2O_2. *E. coli* were suspended in Milli-Q water and natural water having the characteristics described in Table 2. Hematite concentration 0.6 mg/L, H_2O_2: 10 mg/L. Experiments were conducted under simulated solar light and performed in triplicate (the standard error was found to be of ~5%).

$^{\bullet}OH$, thus enhancing bacterial inactivation. According to Spuhler et al. [6], the presence of resorcinol during a photo-Fenton reaction for *E. coli* inactivation enhanced the disinfection rate when compared with that founded without organic matter. They suggested the presence of photo-active Fe^{3+} or Fe^{2+}-resorcinol complexes which may favour the process. In general, the NOM is composed of organic ligands such as fulvic acids and smaller carboxylic and dicarboxylic acids able to form Fe^{3+} complexes which, under light, reduce Fe^{3+} and generate complex with Fe^{2+} and ligand radicals as shown in the next equation [4,6]:

$$Fe^{3+}{-}(L)_n + h\nu \rightarrow Fe^{2+}{-}(L)_{n-1} + L_{ox}{}^{\bullet} \quad (24)$$

Both Fe^{2+} and ligand radicals can react with O_2 leading to the formation of ROS, and the concomitant reaction of Fe^{2+} with H_2O_2 leads to the regeneration of Fe^{3+} and the production of $^{\bullet}OH$ (Eq. (19)). Thus, Fe^{3+} organo-complexes play an important role for the efficiency of photo-Fenton systems.

Finally, no bacterial reactivation and/or growth was observed for the photocatalytic semiconducting and heterogeneous photo-Fenton action of hematite in natural water.

3.5. Influence of iron concentration on bacterial inactivation by hematite-based heterogeneous photo-Fenton

Bacterial inactivation by hematite-based photo-Fenton was evaluated employing three iron concentrations (0.6, 2.3, and 3.8 mg/L). Fig. 8 shows that complete bacterial inactivation was achieved in all cases before 90 min of treatment. Considering the loss of bacteria cultivability at 60 min of treatment, it is evident that bacterial inactivation was dependent of the semiconductor concentration and a liner relationship between hematite concentration and loss of cultivability was observed in this range of concentrations (Fig. 8). Bacterial inactivation kinetics increased with the catalyst dosage, due to the more active iron sites on the catalyst surface, accelerating the decomposition of H_2O_2 and leading to an increase in the number of $^{\bullet}OH$ radicals that obtain bacterial inactivation. The consumption of H_2O_2 in 120 min of treatment, for 0.6, 2.3, and 3.8 mg/L of Fe^{3+} were 1.0, 1.4, and 2.1 mg/L respectively. These results show that low ranges of concentration of hematite

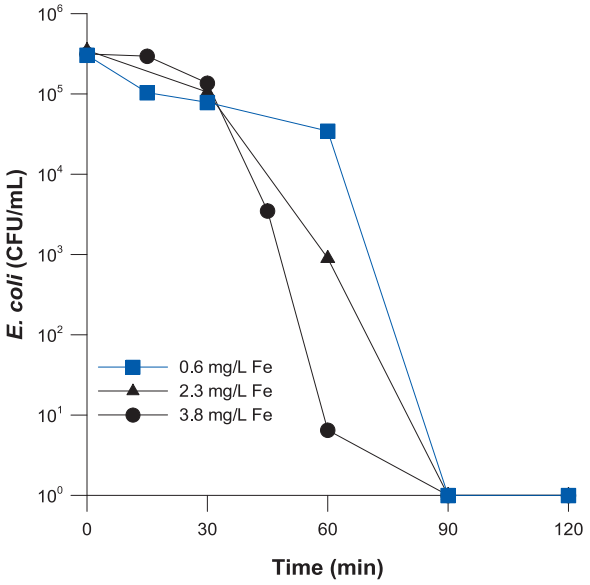

Fig. 8. *E. coli* inactivation under hematite-based photo-Fenton process with different concentrations of Fe^{3+}: 0.6 mg/L, 2.6 mg/L, and 3.8 mg/L. H_2O_2: 10 mg/L. Experiments were conducted under simulated solar light and performed in triplicate (the standard error was found to be of ~5%).

(0.6–3.8) in heterogeneous photo-Fenton system are adequate to efficiently inactivate *E. coli* without reactivation and/or growth of bacteria under the specific experimental conditions. It is interesting to underline that this range of concentrations is close to the concentration found in some lakes, rivers, and ground waters and is low compared with the concentration of iron oxides used for the transformation of organic molecules in aquatic systems (100–500 mg/L of iron oxides) [13,24,68].

4. Conclusions

Our study demonstrated that heterogeneous photo-Fenton processes catalyzed by low concentration of iron (hydr)oxide particles under sunlight may serve as a disinfection method for waterborne bacteria. In particular, we found that, with the exception of magnetite, all the other iron (hydr)oxides tested were photoactive under sunlight in absence of H_2O_2, these involves semiconductor photocatalysis and/or a photo-redox reactions.

The relative low difference of time necessary to inactivate bacteria for photo-assisted hematite and goethite in the absence or presence of H_2O_2 suggest that, from the application point of view, these iron (hydr)oxides can be applied alone as semiconductors to efficiently disinfect water. These results are interesting because the avoidance of H_2O_2 significantly reduces the cost of the treatment. Therefore, the iron (hydr)oxide particles, even those already present in environmental waters, represent low-cost photocatalysts for solar water disinfection. Furthermore, no bacterial reactivation and/or growth was observed for the photocatalytic semiconducting and heterogeneous photo-Fenton action of hematite and goethite, whereas a delayed disinfection effect was observed to continue in the dark for the photo-assisted wüstite treatment.

ESR spin trap technique confirmed that the principal ROS photogenerated for iron (hydr)oxide in the absence or presence of H_2O_2 were $^{\bullet}OH$ and $O_2^{\bullet-}$ radicals. The presence of H_2O_2 in iron (hydr)oxide suspensions promoted a more rapid photo-generation of $^{\bullet}OH$, thus contributing to a more efficient bacterial inactivation.

The components of natural water (*i.e.* NOM and inorganic substances) did not interfere with the photocatalytic semiconducting action of hematite to bacterial inactivation. However, these components enhance the bacterial inactivation by heterogeneous photo-Fenton action of hematite. In particular, NOM enhances the complexation and solubilization of iron, which, in turn, may favour the process. No reactivation and/or growth of bacteria was observed for the photocatalytic semiconducting and heterogeneous photo-Fenton action of hematite in natural water.

Conclusively, our results demonstrated, for the first time, that low concentration of (hydr)oxides (0.6 mg/L) acting both as photocatalytic semiconductors or catalysts of the heterogeneous photo-Fenton process at neutral pH, may provide a useful strategy for efficiently inactivate *E. coli* without reactivation and/or growth. This is important for the economic viability of the treatments because the levels of iron encountered in environmental waters are close to this iron concentration.

Acknowledgements

The authors wish to thank the Swiss National Science Foundation for financial support through the program "Research partnership with developing countries" Project No. IZ70Z0_131312/1-2. We thank Stefanos Giannakis for the English correction.

References

[1] J. Brame, Q. Li, P.J.J. Alvarez, Nanotechnology-enabled water treatment and reuse: emerging opportunities and challenges for developing countries, Trends Food Sci. Technol. 22 (2011) 618–624.
[2] P. Aldhous, The world's forgotten crisis, Nature 422 (2003) 251.
[3] A. Safarzadeh-Amiri, J.R. Bolton, S.R. Cater, The use of iron in advanced oxidation processes, J. Adv. Oxid. Technol. 1 (1996) 18–26.
[4] J.J. Pignatello, E. Oliveros, A. MacKay, Advanced oxidation processes for organic contaminant destruction based on the fenton reaction and related chemistry, Crit. Rev. Environ. Sci. Technol. 36 (2006) 1–84.
[5] A.-G. Rincón, C. Pulgarin, Comparative evaluation of Fe^{3+} and TiO_2 photoassisted processes in solar photocatalytic disinfection of water, Appl. Catal. B: Environ. 63 (2006) 222–231.
[6] D. Spuhler, J. Andrés Rengifo-Herrera, C. Pulgarin, The effect of Fe^{2+}, Fe^{3+}, H_2O_2 and the photo-Fenton reagent at near neutral pH on the solar disinfection (SODIS) at low temperatures of water containing *Escherichia coli* K12, Appl. Catal. B: Environ. 96 (2010) 126–141.
[7] C. Ruales-Lonfat, N. Benítez, A. Sienkiewicz, C. Pulgarín, Deleterious effect of homogeneous and heterogeneous near-neutral photo-Fenton system on *Escherichia coli*. Comparison with photo-catalytic action of TiO_2 during cell envelope disruption, Appl. Catal. B: Environ. 160–161 (2014) 286–297.
[8] J. Rodríguez-Chueca, A. Mediano, M.P. Ormad, R. Mosteo, J.L. Ovelleiro, Disinfection of wastewater effluents with the Fenton-like process induced by electromagnetic fields, Water Res. 60 (2014) 250–258.
[9] J. Rodríguez-Chueca, M.I. Polo-López, R. Mosteo, M.P. Ormad, P. Fernández-Ibáñez, Disinfection of real and simulated urban wastewater effluents using a mild solar photo-Fenton, Appl. Catal. B: Environ. 150–151 (2014) 619–629.
[10] C. Ruales-Lonfat, A. Varón, J. Barona, A. Moncayo-Lasso, N. Benítez, C. Pulgarìn, Iron-catalyzed low cost solar activated process for drinking water disinfection in Colombian rural areas, Technol. Sustain. Dev. (2013) 1–16.
[11] B. Morgan, O. Lahav, The effect of pH on the kinetics of spontaneous Fe(II) oxidation by O_2 in aqueous solution – basic principles and a simple heuristic description, Chemosphere 68 (2007) 2080–2084.
[12] J.P. Jolivet, C. Chaneac, E. Tronc, Iron oxide chemistry. From molecular clusters to extended solid networks, Chem. Commun. (Camb.) 338 (2004) 481–487.
[13] J. He, X. Tao, W.H. Ma, J.C. Zhao, Heterogeneous photo-fenton degradation of an azo dye in aqueous H_2O_2/iron oxide dispersions at neutral pHs, Chem. Lett. (2002) 86–87.
[14] R. Matta, K. Hanna, S. Chiron, Fenton-like oxidation of 2,4,6-trinitrotoluene using different iron minerals, Sci. Total Environ. 385 (2007) 242–251.
[15] X. Xue, K. Hanna, N. Deng, Fenton-like oxidation of Rhodamine B in the presence of two types of iron (II, III) oxide, J. Hazard. Mater. 166 (2009) 407–414.
[16] S. Shin, H. Yoon, J. Jang, Polymer-encapsulated iron oxide nanoparticles as highly efficient Fenton catalysts, Catal. Commun. 10 (2008) 178–182.
[17] F. Mazille, A. Moncayo-Lasso, D. Spuhler, A. Serra, J. Peral, N.L. Benítez, C. Pulgarin, Comparative evaluation of polymer surface functionalization techniques before iron oxide deposition. Activity of the iron oxide-coated polymer films in the photo-assisted degradation of organic pollutants and inactivation of bacteria, Chem. Eng. J. 160 (2010) 176–184.
[18] X. Lv, Y. Xu, K. Lv, G. Zhang, Photo-assisted degradation of anionic and cationic dyes over iron(III)-loaded resin in the presence of hydrogen peroxide, J. Photochem. Photobiol. A: Chem. 173 (2005) 121–127.

[19] D. Tabet, M. Saidi, M. Houari, P. Pichat, H. Khalaf, Fe-pillared clay as a Fenton-type heterogeneous catalyst for cinnamic acid degradation, J. Environ. Manag. 80 (2006) 342–346.
[20] J.R. Chueca, R. Mosteo, M.P. Ormad, N. Miguel, J.L. Ovelleiro, Heterogeneous fenton and photofenton processes for disinfection of treated urban wastewater, Tecnol. Agua 32 (2012) 72–77.
[21] R.M. Cornell, U. Schwertmann, The Iron Oxides: Structure, Properties, Reactions, Ocurrences and Uses, VCH, Weinheim, 2003, ISBN 3-527-30274-3.
[22] P. Xu, G.M. Zeng, D.L. Huang, C.L. Feng, S. Hu, M.H. Zhao, C. Lai, Z. Wei, C. Huang, G.X. Xie, Z.F. Liu, Use of iron oxide nanomaterials in wastewater treatment: a review, Sci. Total Environ. 424 (2012) 1–10.
[23] Z. Zhangl, C. Boxall, G.H. Kelsall, Photoelectrophoresis of colloidal iron oxides 1. Hematite (α-Fe_2O_3), Colloids Surf. A: Physicochem. Eng. Asp. 73 (1993) 145–163.
[24] R. Andreozzi, V. Caprio, R. Marotta, Iron(III) (hydr)oxide-mediated photooxidation of 2-aminophenol in aqueous solution: a kinetic study, Water Res. 37 (2003) 3682–3688.
[25] B. Yuan, J. Xu, X. Li, M.-L. Fu, Preparation of Si–Al/α-FeOOH catalyst from an iron-containing waste and surface-catalytic oxidation of methylene blue at neutral pH value in the presence of H_2O_2, Chem. Eng. J. 226 (2013) 181–188.
[26] H.-H. Huang, M.-C. Lu, J.-N. Chen, Catalytic decomposition of hydrogen peroxide and 2-chlorophenol with iron oxides, Water Res. 35 (2001) 2291–2299.
[27] J.I. Nieto-Juarez, T. Kohn, Virus removal and inactivation by iron (hydr)oxide-mediated Fenton-like processes under sunlight and in the dark, Photochem. Photobiol. Sci. 12 (2013) 1596–1605.
[28] B. Asadishad, S. Ghoshal, N. Tufenkji, Short-term inactivation rates of selected Gram-positive and Gram-negative bacteria attached to metal oxide mineral surfaces: role of solution and surface chemistry, Environ. Sci. Technol. 47 (2013) 5729–5737.
[29] B.M. Pecson, L. Decrey, T. Kohn, Photoinactivation of virus on iron-oxide coated sand: enhancing inactivation in sunlit waters, Water Res. 46 (2012) 1763–1770.
[30] E. Cabiscol, J. Tamarit, J. Ros, Oxidative stress in bacteria and protein damage by reactive oxygen species, Int. Microbiol. 3 (2000) 3–8.
[31] R.M. Cornell, U. Schwertmann, Iron Oxides in the Laboratory: Preparation and Characterization, 2000, ISBN 3527296697.
[32] M.L. Cartron, S. Maddocks, P. Gillingham, C.J. Craven, S.C. Andrews, Feo – transport of ferrous iron into bacteria, Biometals 19 (2006) 143–157.
[33] S.C. Andrews, A.K. Robinson, F. Rodriguez-Quinones, Bacterial iron homeostasis, FEMS Microbiol. Rev. 27 (2003) 215–237.
[34] H.G. Upritchard, J. Yang, P.J. Bremer, I.L. Lamont, A.J. McQuillan, Adsorption to metal oxides of the *Pseudomonas aeruginosa* siderophore pyoverdine and implications for bacterial biofilm formation on metals, Langmuir 23 (2007) 7189–7195.
[35] W. Köster, ABC transporter-mediated uptake of iron, siderophores, heme and vitamin B12, Res. Microbiol. 152 (2001) 291–301.
[36] B. Sulzberger, H. Laubscher, Reactivity of various types of iron(III) (hydr)oxides towards light-induced dissolution, Mar. Chem. 50 (1995) 103–115.
[37] T.D. Waite, F.M.M. Morel, Photoreductive dissolution of colloidal iron oxides in natural waters, Environ. Sci. Technol. 18 (1984) 860–868.
[38] L. Durães, B.F.O. Costa, J. Vasques, J. Campos, A. Portugal, Phase investigation of as-prepared iron oxide/hydroxide produced by sol–gel synthesis, Mater. Lett. 59 (2005) 859–863.
[39] C.V. Santilli, M. Onillon, J.P. Bonnet, Influence of the elaboration and dehydration conditions of Fe(III) hydrous oxides on the characteristics of resulting α-Fe_2O_3 powders, Ceram. Int. 16 (1990) 89–97.
[40] S.-K. Kwon, S. Suzuki, M. Saito, Y. Waseda, Atomic-scale structure and morphology of ferric oxyhydroxides formed by corrosion of iron in various aqueous media, Corros. Sci. 48 (2006) 3675–3691.
[41] P. Cambier, Infrared study of goethites of varying crystallinity and particle size. I: Interpretation of hydroxyl and lattice vibration frequencies, Clay Miner. 21 (1986) 191–200.
[42] C. Wang, H. Liu, Z. Sun, Heterogeneous photo-Fenton reaction catalyzed by nanosized iron oxides for water treatment, Int. J. Photoenergy 2012 (2012) 1–10.
[43] S. Lee, J. Oh, Y. Park, Degradation of phenol with fenton-like treatment by using heterogeneous catalyst (modified iron oxide) and hydrogen peroxide, Bull. Korean Chem. Soc. 27 (2006) 489–494.
[44] P.J. Vikesland, A.M. Heathcock, R.L. Rebodos, K.E. Makus, Particle size and aggregation effects on magnetite reactivity toward carbon tetrachloride, Environ. Sci. Technol. 41 (2007) 5277–5283.
[45] Z.-X. Sun, F.-W. Su, W. Forsling, P.-O. Samskog, Surface characteristics of magnetite in aqueous suspension, J. Colloid Interface Sci. 197 (1998) 151–159.
[46] V.M. Buzmakov, A.F. Pshenichnikov, On the structure of microaggregates in magnetite colloids, J. Colloid Interface Sci. 182 (1996) 63–70.
[47] I.S.X. Pinto, P.H.V.V. Pacheco, J.V. Coelho, E. Lorençon, J.D. Ardisson, J.D. Fabris, P.P. de Souza, K.W.H. Krambrock, L.C.A. Oliveira, M.C. Pereira, Nanostructured δ-FeOOH: an efficient Fenton-like catalyst for the oxidation of organics in water, Appl. Catal. B: Environ. 119–120 (2012) 175–182.
[48] R.C.C. Costa, M.F.F. Lelis, L.C.A. Oliveira, J.D. Fabris, J.D. Ardisson, R.R.V.A. Rios, C.N. Silva, R.M. Lago, Novel active heterogeneous Fenton system based on $Fe_{3-x}M_xO_4$ (Fe, Co, Mn, Ni): the role of M^{2+} species on the reactivity towards H_2O_2 reactions, J. Hazard. Mater. 129 (2006) 171–178.
[49] S.-H. Kong, R.J. Watts, J.-H. Choi, Treatment of petroleum-contaminated soils using iron mineral catalyzed hydrogen peroxide, Chemosphere 37 (1998) 1473–1482.
[50] D. Beydoun, R. Amal, G.K.C. Low, S. McEvoy, Novel photocatalyst: titania-coated magnetite. Activity and photodissolution, J. Phys. Chem. B 104 (2000) 4387–4396.
[51] J.C. Chou, S.A. Lin, C.Y. Lee, J.Y. Gan, Effect of bulk doping and surface-trapped states on water splitting with hematite photoanodes, J. Mater. Chem. A 1 (2013) 5908–5914.
[52] D. Beydoun, R. Amal, G. Low, S. McEvoy, Occurrence and prevention of photodissolution at the phase junction of magnetite and titanium dioxide, J. Mol. Catal. A: Chem. 180 (2002) 193–200.
[53] P.C. Maness, S. Smolinski, D.M. Blake, Z. Huang, E.J. Wolfrum, W.A. Jacoby, Bactericidal activity of photocatalytic TiO_2 reaction: toward an understanding of its killing mechanism, Appl. Environ. Microbiol. 65 (1999) 4094–4098.
[54] P.M. Borer, B. Sulzberger, P. Reichard, S.M. Kraemer, Effect of siderophores on the light-induced dissolution of colloidal iron(III) (hydr)oxides, Mar. Chem. 93 (2005) 179–193.
[55] J. Ndounla, D. Spuhler, S. Kenfack, J. Wéthé, C. Pulgarin, Inactivation by solar photo-Fenton in pet bottles of wild enteric bacteria of natural well water: absence of re-growth after one week of subsequent storage, Appl. Catal. B: Environ. 129 (2013) 309–317.
[56] G.R. Buettner, R.P. Mason, Spin-trapping methods for detecting superoxide and hydroxyl free-radicals in-vitro and in-vivo, Methods Enzymol. 186 (1990) 127–133.
[57] A.B. Stefaniak, C.J. Harvey, V.C. Bukowski, S.S. Leonard, Comparison of free radical generation by pre- and post-sintered cemented carbide particles, J. Occup. Environ. Hyg. 7 (2010) 23–34.
[58] J. Xu, N. Sahai, C.M. Eggleston, M.A.A. Schoonen, Reactive oxygen species at the oxide/water interface: formation mechanisms and implications for prebiotic chemistry and the origin of life, Earth Planet. Sci. Lett. 363 (2013) 156–167.
[59] P. Mazellier, M. Bolte, Heterogeneous light-induced transformation of 2,6-dimethylphenol in aqueous suspensions containing goethite, J. Photochem. Photobiol. A: Chem. 132 (2000) 129–135.
[60] Y. Xu, M.A.A. Schoonen, The absolute energy positions of conduction and valence bands of selected semiconducting minerals, Am. Mineral. 85 (2000) 543–556.
[61] I. TitanPE Technologies, http://www.naprotec.be/uploaded/Sterilization%20by%20Titanium%20and%20Silver%20coatings.pdf, Shanghai, 2011.
[62] F. Widdel, S. Schnell, S. Heising, A. Ehrenreich, B. Assmus, B. Schink, Ferrous iron oxidation by anoxygenic phototrophic bacteria, Nature 362 (1993) 834–836.
[63] M. Brasca, S. Morandi, R. Lodi, A. Tamburini, Redox potential to discriminate among species of lactic acid bacteria, J. Appl. Microbiol. 103 (2007) 1516–1524.
[64] J. Kiwi, M. Gratzel, Light-induced hydrogen formation and photo-uptake of oxygen in colloidal suspensions of α-FE_2O_3, J. Chem. Soc.: Faraday Trans. I 83 (1987) 1101–1108.
[65] M.D. Paciolla, G. Davies, S.A. Jansen, Generation of hydroxyl radicals from metal-loaded humic acids, Environ. Sci. Technol. 33 (1999) 1814–1818.
[66] S.K. Han, T.M. Hwang, Y. Yoon, J.W. Kang, Evidence of singlet oxygen and hydroxyl radical formation in aqueous goethite suspension using spin-trapping electron paramagnetic resonance (EPR), Chemosphere 84 (2011) 1095–1101.
[67] J. Wenk, U. Von Gunten, S. Canonica, Effect of dissolved organic matter on the transformation of contaminants induced by excited triplet states and the hydroxyl radical, Environ. Sci. Technol. 45 (2011) 1334–1340.
[68] J. He, W. Ma, W. Song, J. Zhao, X. Qian, S. Zhang, J.C. Yu, Photoreaction of aromatic compounds at —FeOOH/H_2O interface in the presence of H_2O_2: evidence for organic-goethite surface complex formation, Water Res. 39 (2005) 119–128.